Available online at www.sciencedirect.com
ScienceDirect
Analytica Chimica Acta 582 (2007) 1–9
ANALYTICA CHIMICA ACTA
www.elsevier.com/locate/aca

Matrix-assisted laser desorption/ionization (MALDI) mechanism revisited

Wei Chao Chang [a], Ling Chu Lora Huang [a], Yi-Sheng Wang [a], Wen-Ping Peng [a], Huan Cheng Chang [b], Nien Yeen Hsu [c], Wen Bin Yang [a], Chung Hsuan Chen [a,*]

[a] *Genomics Research Center, Academia Sinica, Taipei, Taiwan*
[b] *Institute of Atomic & Molecular Sciences, Academia Sinica, Taipei, Taiwan*
[c] *Department of Chemistry, National Taiwan University, Taipei 10674, Taiwan*

Received 14 July 2006; received in revised form 24 August 2006; accepted 24 August 2006
Available online 9 September 2006

Abstract

Although matrix-assisted laser desorption/ionization (MALDI) was developed more than a decade ago and broad applications have been successfully demonstrated, detailed mechanism of MALDI is still not well understood. Two major models; namely photochemical ionization (PI) and cluster ionization (CI) mechanisms have been proposed to explain many of experimental results. With the photochemical ionization model, analyte ions are considered to be produced from a protonation or deprotonation process involving an analyte molecule colliding with a matrix ion in the gas phase. With the cluster ionization model, charged particles are desorbed with a strong photoabsorption by matrix molecules. Analyte ions are subsequently produced by desolvation of matrix from cluster ions. Nevertheless, many observations still cannot be explained by these two models. In this work, we consider a pseudo proton transfer process during crystallization as a primary mechanism for producing analyte ions in MALDI. We propose an energy transfer induced disproportionation (ETID) model to explain the observation of an equal amount of positive and negative ions produced in MALDI for large biomolecules. Some experimental results are used for comparisons of various models.

Keywords: Matrix-assisted laser desorption/ionization; Ionization mechanism; Biopolymer ion

1. Introduction

Matrix-assisted laser desorption/ionization (MALDI) [1,2] and electrospray ionization (ESI) [3] have become the most valuable methods for producing high mass ions for mass spectrometry analysis. MALDI has the advantages of producing mostly singly charged parent ions [4] so that the spectra are more suitable for mixture analysis. It has been broadly used for most proteomic analysis [5] without the need of a liquid chromatography for pre-separation. In addition to proteins and peptides, MALDI has also been used for the analysis of oligonucleotides [6,7], polysaccharides [8,9], glycoproteins [10], glycolipids [11] and synthetic polymers [12]. Due to the rapid analysis speed, MALDI has also been extensively used for oligonucleotide sequencing [13,14], disease diagnosis [15] and single nucleotide polymorphism (SNP) analysis [16]. MALDI has demonstrated great impact on biomedical [17], chemical [18] and pharmaceutical [19] industries. Despite the impressive progress in MALDI applications, MALDI is notoriously known for poor reproducibility [20] so that quantitative measurement is quite difficult. In addition, the mass resolution of a linear time-of-flight MALDI mass spectrometer is usually low for molecules with a high mass to charge ratio (*M*/*Z*) due to the broad energy spread of these large molecules [21]. However, a reflectron time-of-flight MALDI mass spectrometer seldom works well for very large oligonucleotide molecular ions due to the existence of metastable states [22]. Although MALDI has had great success in measuring protein and small to medium size oligonucleotides, MALDI is still not very useful for routine analysis of very large polysaccharides [23], glycoproteins [24], nucleic acids [25] and organic polymers [26] due to the lack of right matrices. In order to overcome the barrier of low reproducibility and poor mass resolution, understanding the MALDI mechanism is critically important. Although thousands of papers have been published on MALDI applications, the detailed mechanism is more or less not known. Indeed, there is still no agreement on a simple model for the MALDI process.

* Corresponding author. Tel.: +886 2 27899930; fax: +886 2 27899931.
E-mail address: winschen@gate.sinica.edu.tw (C.H. Chen).

0003-2670/$ – see front matter © 2006 Elsevier B.V. All rights reserved.
doi:10.1016/j.aca.2006.08.062

In 1992, Ehring et al. [27] proposed a photochemical ionization model for the MALDI process. Photoionization of matrix molecules is considered as the primary mechanism for subsequent ionization of an analyte ion in the gas phase. Energy pooling, and multiphoton absorption are the major processes to lead to the photoionization of matrix molecule. An analyte ion is produced by protonation or deprotonation from a collision process with a matrix ion to form a positive or a negative analyte ion [28]. Since the sum energy of two nitrogen laser photons is 7.36 eV which is lower than the ionization potential of most matrix molecules, two-photon ionization of a matrix molecule was considered as unlikely [29]. With most MALDI experiments performed with the laser radiances from 10^6 to 10^7 W cm^{-2}, the ionization efficiency should be quite low for a three photon ionization process. Due to the limited number of excited matrix molecules produced, energy pooling processes should not be very efficient to produce a large number of matrix ions. In addition, this model fails to explain many phenomena observed in MALDI processes such as matrix suppression effect [30], "sweet spots" [31] and high ratios of polymer ions to monomer ions.

Matrix suppression effect has been observed for small analytes with low molar ratios of matrix to analyte molecules. With photochemical ionization model, all analyte ions have to come from collision processes between neutral analyte molecules and protonated or deprotonated matrix molecules. Since the time allowed for the proton transfer process is less than 1 μs and the quantity of analyte molecules is significantly less than that of matrix molecules, it is difficult to explain matrix suppression by the photochemical ionization model. If analyte ions have to be produced in collision processes in the gas phase, MALDI signal should be irrelevant to the crystallization pattern and sweet spots should not be observed. Production of a large amount of polymer ions within 1 μs after the desorption laser pulse is also difficult to be explained with the photochemical ionization model.

The production of analyte ions in MALDI with a gas phase photochemical ionization model was often considered to involve a two-step ionization process [32]. The first step is to produce primary matrix ions and analyte ions are subsequently produced from the interaction of matrix ions with analyte molecules. In addition to energy pooling and multiphoton ionization for matrix ion production, excited-state proton transfer [33], disproportionation reaction [34] and thermal ionization [35] have all been considered as possible processes to produce matrix ions. Desorption of preformed ions has also been proposed and studied by Lehman et al. [36]. IR spectroscopy has been used to indicate the existence of preformed ions. However, it has been more or less limited to explain results from MALDI of organometallic and bio-metallic compounds with a low ionization potential. None of the above processes have been considered a dominant process to produce analyte ions. For secondary ionization, proton transfer and electron transfer [37] with matrix ions are considered as the primary processes to produce analyte ions. However, electron transfer processes to produce analyte ions usually only occurs if the ionization potential of the matrix molecule is higher than that of the analyte molecule.

The photochemical ionization model has been broadly accepted since the discovery of MALDI although it fails to explain many experimental observations. Recently, Karas and co-workers proposed a new cluster ionization (CI) mechanism [38–40] that is quite different from the photochemical ionization model. The cluster ionization model assumes large protonated analyte polymers exist in the acidic matrix environment. These clusters are desorbed during the laser irradiation. Analyte ions are produced in the gas phase by the desolvation of neutral matrix molecules. This process is similar to the water desolvation for a typical electrospray ionization (ESI) mass spectrometer. With the cluster ionization (CI) model, ion–molecule interactions in gas phase are no longer needed. This model is in agreement with the observation of particles found after MALDI process. A molecular beam experiment also revealed that matrix cluster ions can be obtained by laser excitation indicating that cluster ions could be the precursors of the analyte ion [41]. Nevertheless, it does not prove that most analyte ions are produced from cluster ions. With the cluster ionization model it seems to be difficult to explain the predominant production of mono-charged ions for biomolecules with a broad mass range since ESI produces mostly multiply charged ions for large biomolecules. It is also short of clear explanation on sweet spots and the matrix suppression effect. In this work, we consider a pseudo proton transfer process occurring during the crystallization process for MALDI sample preparation. We consider that a proton from an acidic matrix is dominantly shared with the basic site of a biomolecule as a pseudo proton transfer process. This pseudo proton transfer process in solid can occur between analyte and matrix molecules as well as between analyte molecules. Due to the observation of an equal amount of positive and negative ions of large biomolecules, we further propose an energy transfer induced disproportionation (ETID) model for large analyte ion production. An analyte ion is produced by energy transfer from an excited matrix molecule to an analyte dimer to produce one positive and one negative ion simultaneously. Experimental results from both positive and negative ion spectra for monomer and polymer ions are used for the comparison of various models for the MALDI process.

2. Experimental

2.1. Mass spectrometry facilities

An ABI Voyager time-of-flight mass spectrometer (Foster City, CA, USA) was used for obtaining MALDI mass spectra. Delayed ion extraction was available for optimizing ion signals. However, the delayed time was generally fixed at 10 ns and the pulsed voltage was fixed at 10% of the biased voltage on the sample plate. Ion energy can be varied from 0 to 25 keV and the biased voltage of the microchannel plate detector was in general set at 900 V. In this work, the laser fluence was frequently monitored using a Laser Technik power meter (PEM 100 Laser Technik Berlin, Germany). The laser beam diameter on the sample target was measured as ∼100 μm. The laser fluence used is in the range of 50–200 mJ cm^{-2}.

A home-made ion trap particle mass spectrometer with the capability of measuring mass to charge ratio up to 10^{10} was used to estimate the weight of desorbed matrix particles. The

details of the facility and experimental steps were published before [42,43]. The following briefly describes the experiments regarding the measurement of matrix clusters. Charged cluster particles were introduced into the ion trap through the gap between the ring and end-cap electrodes. A frequency-tripled pulsed Nd:YAG laser (355 nm, 200 μJ) was used to irradiate the sample surface. Desorbed charged particles were captured by the ion trap driven by a home-built audio frequency power amplifier in a bipolar mode. Particles were analyzed one at a time under a high vacuum condition (pressure $\sim 1 \times 10^{-6}$ Torr). To observe the particle's oscillatory motion inside the ion trap, the trapped particle was illuminated with an argon ion laser beam (488 nm and 100 mW) going through the gap between the ion trap electrodes. The resulting scattered laser light was detected by a charge-coupled device (CCD) camera. By properly adjusting the trap driving frequency, a single particle was isolated and the trajectory of the particle's motion projected on the radial plane shows a stationary star pattern on the CCD camera. Mass-to-charge ratios of the trapped particle were deduced from its secular frequencies in the radial coordinate. The absolute mass determination was accomplished using an electron stepping procedure.

2.2. Chemicals and reagents

Bovin serum albumin (BSA, 95%), cytochrome *C* (97%), trypsinogen, insulin myoglobin, 2,5-dihydroxybenzoic acid (2,5-DHB), sinapinic acid (SA), α-cyano-4-hydroxycinnamic acid (CHCA) and 3-HPA were purchased from Sigma Inc. (Saint Louis, USA); ammonium acetate (NH_4OAc), acetonitrile (ACN), synthetic peptides with the sequence of AAAKAAAK and oligonucleotide with the sequence of GATCGATCGATCGATCGATC were purchased from Merck (Darmstadt, Germany).

2.3. MALDI sample preparation

Three different approaches were used to prepare MALDI samples. One is the standard method for MALDI sample preparation with the mixed matrix/analyte solution droplet dried in air on the sample plate. With this method, inhomogeneous sample distribution and "sweet spots" can be expected. The second approach is to have a rapid crystallization process by using vacuum pumping. Chemical distribution on each sample spot is much more homogeneous than the drying process in air. The third method is just mixing matrix and analyte powder together in a ball mill and grinding for a few minutes.

For peptide, protein and oligonucleotide samples, each compound was prepared to 1 nmol μL^{-1} as a stock concentration then diluted in 50% ACN to the desired concentration for analysis. Matrix of 2,5-DHB and 3-HPA were dissolved in 50% ACN to a final concentration of 50 nmol μL^{-1}. Each compound and matrix were mixed as equal volume (1 μL:1 μL) and deposited onto a 0.2-cm^2 sample plate area. The mixture solution was allowed to air dry or vacuum dry prior to analysis.

For mass measurement of matrix clusters, nanometer-size matrix clusters were prepared by a saturated solution of matrix in the solvent mixture (70% acetonitrile and 30% water) and subsequently placed on a Si wafer surface to form crystalline.

3. Results and discussions

We recently observed nearly identical mass spectra for both positive and negative ion mode for protein and oligonucleotide. Some typical results are shown in Fig. 1. The amplitudes for monomer and polymer ions with different polarities are the same within experimental fluctuation. We have examined several different proteins including insulin, cytochrome *c*, myoglobin, bovine serum albumin (BSA) and various size oligonucleotides. Equal signal amplitudes for different polarities were obtained. These results are not agreeable with the conventional expectation that more positive ions than negative ions would be produced during a MALDI process of proteins especially with basic amino acids. On the other hand, stronger negative ion signals than the corresponding positive ion signals are expected for oligonucleotide since oligonucleotide molecules are often negatively charged with alkali metal as counter ions. These observations are difficult to be interpreted by either the photochemical ionization (PI) model or the cluster ionization (CI) model. For the photochemical ionization model, the mechanisms producing positive and negative analyte ions are expected to be different. Thus it is very unlikely to produce equal number of both positive and negative ions for MALDI for so many different kinds of biomolecules. For the cluster ionization model, ions are considered to be produced as desorbed cluster ions with a desolvation process to eventually produce mono-charged analyte ions. Details on the production of mono-charged analyte ions from a cluster ion with desolvation were little discussed [38–40]. In this work, we consider a pseudo proton transfer process during crystallization as the primary process to produce analyte ions in MALDI. For the explanation of the equal production of positive and negative ions, we propose a model of energy transfer induced disproportionantion (ETID) as a primary MALDI mechanism for large analyte ion production. A simplified picture for this model is shown in Fig. 2. Two analyte molecules share an active proton through hydrogen bonding in the solid phase. A "nearby" matrix molecule is closely coupled to the bonding proton that is shared by the two analyte molecules. With absorption of a laser photon by the "nearby" matrix molecule, the excited matrix molecule can transfer its energy through short range energy transfer mechanism to an analyte dimer to produce disproportionation which leads to one protonated and one deprotonated analyte ion simultaneously. We consider the short range energy transfer from the "nearby" matrix molecule to the proton sharing bonding as essential to produce the equal number of positive and negative analyte ions. The distance between the analyte dimer and the "nearby" matrix molecule should be within a few nanometers. In the following, we will discuss various phenomena observed in MALDI with three different models.

3.1. Matrix selection, crystallization and "sweet spots"

Up to now, there are about a dozen successful matrix molecules enabling production to obtain strong MALDI signals

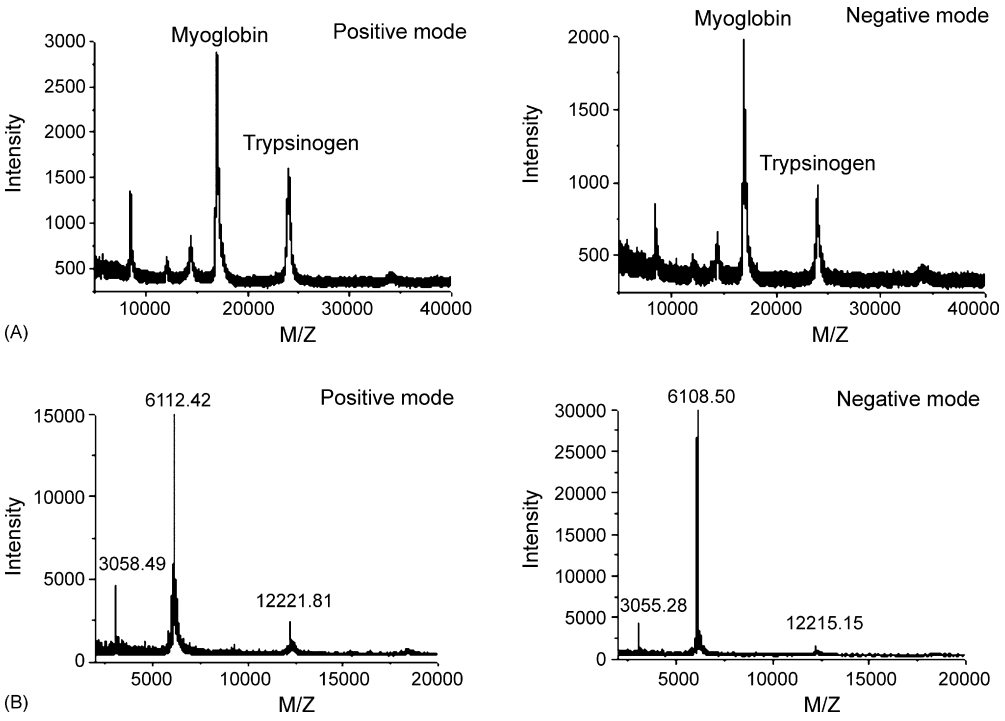

Fig. 1. MALDI-TOF mass spectra in both positive and negative modes for proteins and oligonucleotides. (A) Mixtures of trypsinogen and myoglobin with sinapinic acid as matrix. The analyte quantity was 10 pmol for each biomolecule and the molar ratio of matrix to each biomolecule was 1×10^4. Samples were prepared with a regular drying process in air. The laser fluences used were 67 mJ cm^{-2}. Please note signal intensities from corresponding positive and negative polymer ions are about the same within experimental fluctuation. (B) MALDI-TOF mass spectra in both positive and negative modes for oligonucleotide. The quantities of oligonucletide and matrix (3-HPA) were 50 pmol and 200 nmol, respectively. The size of oligonucleotide was 20 nucleotides. The sequence of this oligonucleotide is $(GATC)_5$. The crystallization process was either through air drying or vacuum drying. The laser fluence used was 102 mJ cm^{-2}. The signal amplitudes for both positive and negative monomer ions are about the same.

from protein and peptide. There are less than five matrix compounds working well for large oligonucleotide. "Good" matrix compounds for proteins are often used for polysaccharide. Nevertheless, the efficiency for MALDI of polysaccharide is only about 0.1% or less compared to proteins with a similar mass. The selection of a matrix for different kinds of analyte molecules is very critical. It indicates that the photochemical ionization model is not the primary mechanism for ionization of very large ana-

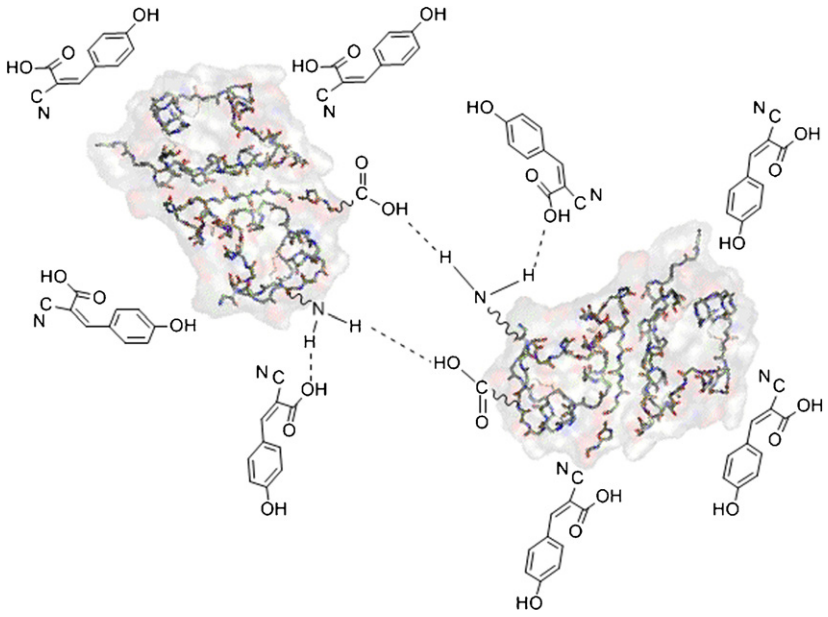

Fig. 2. The schematic of the energy transfer induced disproportionation (ETID) model for the MALDI ionization mechanism. Insulin and α-cyano-4-hydroxycinnamic acid are used as an example for simulating the proposed ETID model.

lyte molecules. There is evidence to show ion signals produced from very small peptides and polysaccharide ($M < 1000$ Da) are less sensitive to the selection of matrix as long as the different matrix molecules have comparable laser absorption efficiency.

It is well known in MALDI community that "sweet spots" do exist in regular MALDI samples. Analyte ion signals from a "non-sweet spot" compared to the corresponding signals from a "sweet spot" can be only a few percent. Many efforts have been placed on reducing "sweet spots" to increase homogeneity and reproducibility [44]. On the other hand, "sweet spots" were often searched for samples with low MALDI signals. For oligonucleotides larger than 100 nucleotides, search for "sweet spots" is almost essential to obtain decent signals [45]. Although the "sweet spot" effect has been known and studied for a long time, it has seldom been discussed for different MALDI ionization models. Since "sweet spots" only exist in the crystallization form of MALDI samples, it is difficult to use the photochemical ionization model to explain the effect. If analyte ions have to be primarily produced from proton transfer processes in the gas phase, the exact status of the analyte molecule in the solid MALDI sample should have little effect in terms of the production of analyte ions. Most "sweet spots" have clear crystal structure instead of amorphous looking. We prepared MALDI samples from both a regular air dry and rapid vacuum dry processes. Samples from a vacuum dry process usually look more homogeneous and are believed to have little "sweet spots". Mass spectra obtained from samples prepared by a rapid vacuum dry process are often much more reproducible. With 3-hydroxypicolinic acid (3-HPA) as the matrix for oligonucleotide detection, the signals of oligonucleotide ions from regular air dry are higher than the corresponding signals from the vacuum drying process. Similar results were also obtained from BSA samples. Ion signals from BSA are higher from a "sweet spot" than the corresponding signals from a "non-sweet spot".

With the cluster ionization (CI) model, the "sweet spot" effect is difficult to explain unless sweet spots lead to more cluster ions produced. With the proposed energy transfer induced disproportion (ETID) model, it is essential to have matrix molecules "nearby" the analyte complex thus both the crystallization process and matrix selection become critical. Thus, ETID can be used to explain the "sweet spot" effect.

3.2. Polymer ion production

Typical mass spectra of BSA are shown in Fig. 3. They clearly indicate high polymer ions are produced. Tetramer ions with m/z ~264,000 were observed. Nearly all commercial mass spectrometers are equipped with charged particle detectors such as electromultiplier, channeltron and microchannel plates. The principle of these charged particle detectors is based on the ejection of secondary electrons. However, the secondary electron ejection efficiencies for various very large ions are known to be very low [46] but have never been measured. The reason of the low secondary electron ejection efficiency for very large ions is due to the low velocity. With 30 keV of kinetic energy, an ion with m/z 100,000, has a velocity of only 7.6×10^3 m s^{-1} which is equivalent to a He^+ at 1.2 eV. We measured the relative secondary electron ejection efficiencies as a function of the velocity (to be published separately). It was found that secondary electron ejection efficiency is a function of v^n with n higher than 4 for BSA and v represents velocity of ions. With the correlation factors included, the spectrum to reflect the relative populations of these polymer ions is also shown in the lower part of Fig. 3. It clearly indicates that the populations of all differ-

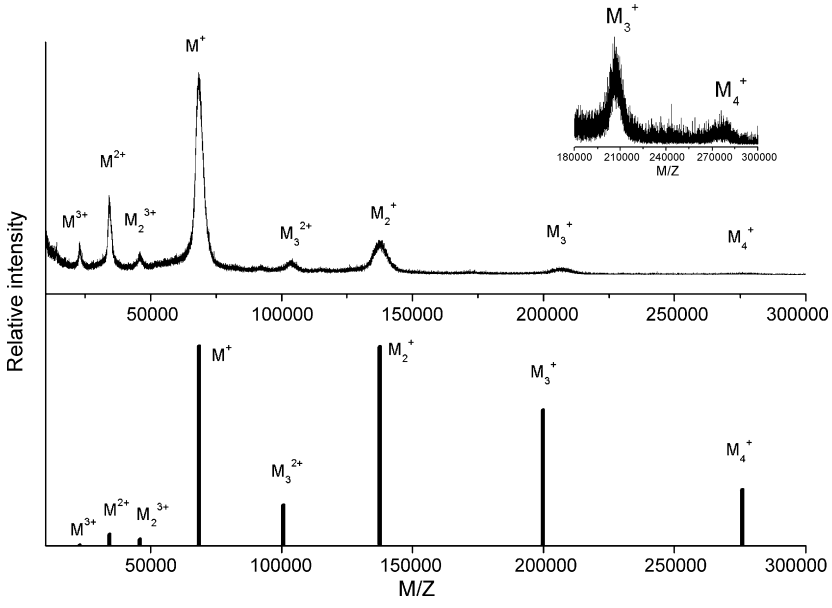

Fig. 3. Polymer positive ion spectrum of BSA with DHB as matrix. The sample was prepared by mixing 2 μL of BSA at 2 μM with 2 μL of DHB at 0.1 M concentration. The sample mixture (1 μL) was taken out for MALDI measurement. The laser fluence used was 67 mJ cm^{-2}. The velocity-correlated spectrum is shown in the lower part of the figure to indicate the high ratio of polymer ions compared to monomer ions. Please note the populations of multiple-charged ions are significantly lower than polymer ions.

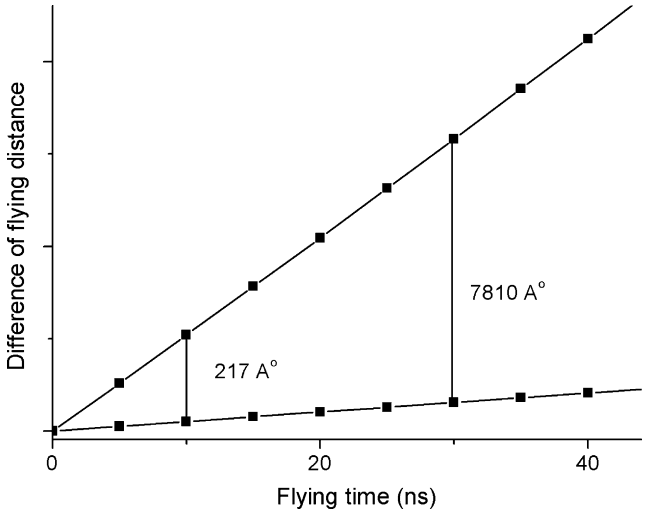

Fig. 4. Calculation of the mean separation of desorbed matrix ions from neutral biomolecules. No delay extraction and no space charge were assumed. The voltage difference between sample plate and the first extraction plate is set as 2500 V and the distance between these two plates was 9 mm. This result indicates the collision time is about 10 ns before the separation becomes too big to have any efficient protonation or deprotonation to occur.

ent size polymer ions are very comparable to the corresponding monomer ions.

The photochemical ionization model is difficult to be used to explain the high population ratio for polymer ions compared to monomer ions. With the assumption of the laser fluence low enough not to produce serious space charge in the desorption plume and no delay extraction device, it should take less than 50 ns to separate desorbed matrix ions from a large neutral analyte molecule by ~1 μm with the voltage difference of 2500 V between the sample plate and the extraction plate (see Fig. 4). Thus the efficient gas phase reaction time to produce analyte ions should be less than 50 ns. Although it is difficult to measure the molecule density in the plume right after desorption, it can be reasonable to assume the local pressure should be less than 1 Torr. If we take the high end of the ion molecular proton exchange reaction cross section as 10^{-14} cm^2 and the average velocity of an analyte molecule as 10^6 cm s^{-1}, the proton transfer probability between matrix ion and neutral analyte molecule to produce protonated analyte ion $(A+H)^+$ or deprotonated ion $(A-H)^-$ can be estimated as

$$P = n\sigma vt = 3 \times 10^{16} \times 0.01\% \times 10^{-14} \times 10^6 \times 50 \times 10^{-9},$$

$$P = 1.5 \times 10^{-3}$$

where n is the number density of analyte molecule in the plume reaction zone, σ the proton transfer cross section, v the relative velocity and t is the reaction time. The molar ratio of analyte to matrix is assumed as 0.01% in a typical MALDI experiment. Although the estimate of protonation of the above equation is not precise, nevertheless, it clearly indicates the number of dimer ion production should be orders of magnitude lower than that of monomer ions. It is nearly impossible to observe higher polymer ions with photochemical ionization model. Insulin 20-mer ions in a MALDI experiment were reported before [47]. The observation of a large number of polymer ions rules out the photochemical ionization process as a primary mechanism for analyte ion production in MALDI. It again indicates that the photochemical ionization model should not be the primary mechanism to produce high analyte polymer ions.

The cluster ionization model proposed by Karas and coworkers [38–40] has not given any detailed discussions on the production of analyte polymer ions. Nevertheless, the assumption of cluster ions as the precursors of mono-charged ions can be extended to the production of polymer ions embedded in the matrix clusters. When the laser fluence is increased, more cluster desorption can be expected. However, the relationship of desorbed clusters versus laser fluence has not been established. In general, higher laser power density tends to more efficiently produce smaller clusters than those produced by lower laser power density with the same laser energies. Since the details of desolvation to produce mono-charged analyte ions in cluster ionization model are still not known, it is impossible to give any prediction of analyte ion production versus laser fluence by the cluster ionization model. However, the cluster ionization model is difficult to explain the equal number of large analyte polymer ions with different polarity produced in the MALDI processes (Fig. 1).

With our proposed pseudo proton transfer process during crystallization in sample preparation, sweet spots, high polymer ratio and high selectivity of matrix can all be explained. Nevertheless, it is still difficult to explain the observation of equal amount of positive and negative ions produced for large proteins and oligonucleotides. During the crystallization process, large biomolecules can have the tendency to form polymers [48]. We thus propose an energy transfer induced disproportionantion (ETID) model. For the ETID model, there are no contradictions from polymer ion data. During the crystallization process, high analyte polymers can be formed. When two analyte polymers share a proton, energy transfer from a "nearby" excited matrix molecule can cause polymer ion production. A concern can be raised regarding the possibility of different sizes of analyte polymers, such as a dimer protein with a monomer protein to share the proton. We consider the proton to have nearly equal possibility to attach to either side of the protein so that the production of both positive and negative polymer ions should be nearly equal due to this heterogeneous sharing of the proton. Take a monomer–dimer complex as an example, a proton to be transferred from a monomer to a dimmer should not be very different from the possible transfer from dimmer to a monomer for large proteins. Thus, equal number of positive and negative polymer ions should be produced.

3.3. Production of mono-charged analyte ions

As described in the above section, it is difficult to clearly explain the production of high polymer ions with the photochemical ionization model since there is not enough time to have enough collisions. On the other hand, the desolvation of matrix molecules by the cluster ionization model may be difficult to justify the predominant mono-charged analyte ion production. With a typical electrospray ionization mass spectrometer, the desolvation process needs to go through a ~10 cm long heating

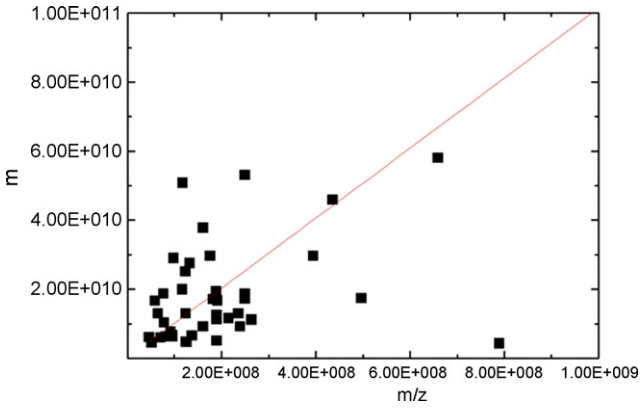

Fig. 5. Mass distribution of sinapinic acid cluster generated by the MALDI process.

zone to get rid of water molecules. In general the desolvation was performed in 1 atm. air pressure so that lots of collision processes can cause more efficient desolvation. With a typical MALDI process, there is only less than 1 μs or 1 cm travel distance (the distance between sample plate and field free zone) for desolvation of matrix molecules. It is orders of magnitude in time difference for desolvation compared to the desolvation in an ESI process. We performed an experiment to measure the desorbed MALDI cluster ions by cell mass spectrometry which is an ion trap mass spectrometer with a low RF frequency to trap an entire cell for mass measurement [49]. The results are shown in Fig. 5. The average mass of matrix cluster is about 10^{10} Da which is equivalent to ~250 nm particle and a cluster of ~50 million matrix molecules. The average charge is obtained as ~100 per particle. Since this work was performed in *m*/*z* preset condition, it precludes the measurement of much smaller clusters [42]. Nevertheless, it indicates nanometer to micrometer size particles did occur during MALDI process. However, the production of particles does not necessary mean the mono-charged ions are primarily produced by desorbed charged particles through a desolvation process. A process to desolvate hundreds to millions of matrix molecules within 1 μs seems very unlikely. With the ETID model, the production of analyte molecules needs the energy transfer of "nearby" matrix molecules. Since it is not easy to have many of these configurations in one analyte–analyte complex, most analyte ions produced should be singly or doubly charged. Greater than triply charged analyte ions should only occur for very large analyte molecules. With this model, the populations of doubly and triply charged ions should be much less than mono-charged ions. Experimental results shown in Fig. 3 agree with this prediction.

3.4. MALDI of small peptides

Both positive and negative ion spectra for MALDI of short peptides with the sequence of AAAKAAAK (M_W 700.84 Da) are shown in Fig. 6 which shows the positive ion signals are slightly higher than the corresponding negative signals. These results are more difficult to be explained by ETID model. For short peptide, it is less likely to trap a nearby matrix molecule for excitation energy transfer to lead to ETID. On the other hand, pseudo proton transfer processes between matrix and peptide can still be an important mechanism to produce peptide ions. Since most peptides are acidic, the production of more positive peptide

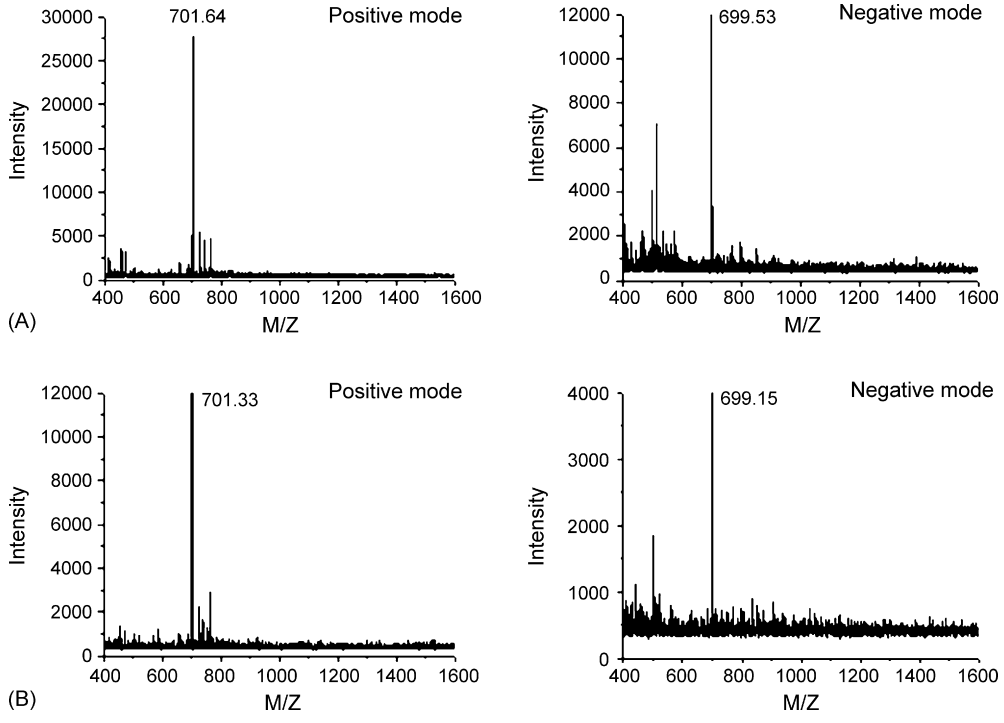

Fig. 6. Positive and negative ion spectra of a peptide with sample preparation by the rapid vacuum dry crystallization process. The amplitudes of positive ion signals are slightly higher than the corresponding negative ion signals. The molar ratio of matrix to peptide is 1000. The laser fluence used was 45 mJ cm^{-2}. (A) Spectra were obtained from a sample dried in air and (B) spectra from a sample with a vacuum drying process.

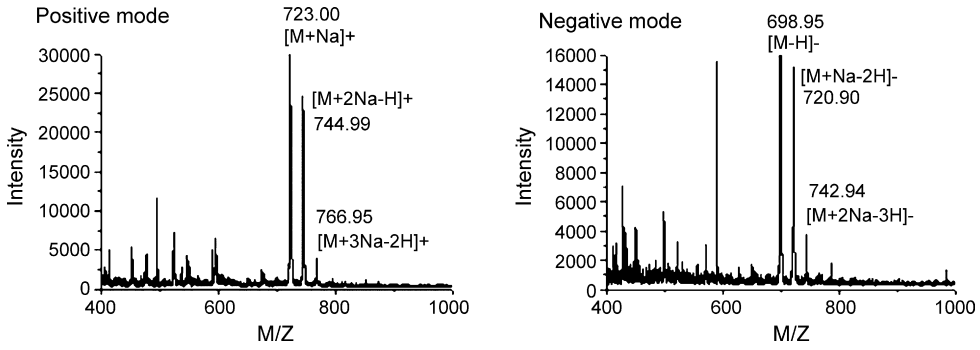

Fig. 7. Positive and negative ion spectra of a peptide with gold nanoparticle. It was found that positive ion signals are slightly higher than the corresponding negative ion signals. The laser fluence used was 102 mJ cm^{-2}. The quantity of nanogold in the sample was 10^{10} particles while the quantity of peptide was 50 nmol. The size of the gold nanoparticle was 23 nm.

ions can also be expected from pseudo proton transfer processes in solid. Nevertheless, it cannot be ruled out that some short peptide ions can be produced in the gas phase as described by the photochemical ionization mechanism. In general, the selection of matrix becomes much less critical for short peptides. Indeed, short peptides can be produced with a short wavelength laser without the need of matrix. We also observed short peptide ions can also be produced with dye molecules as matrix. It seems the major role of the matrix is to absorb laser energy to lead to peptide desorption. The ionization process can be achieved by way of collision in the gas phase. In general, the polymer ion signals compared to monomer ion signals are less for short peptides compared to proteins.

Positive ion signals were much higher than the corresponding negative ion signals with powder matrix. With this powder experiment, it is less likely to have pseudo proton transfer between matrix and analyte molecules. It is also unlikely to have a nearby matrix molecule to lead to ETID to produce positive and negative ions. Thus, the gas phase photochemical ionization mechanism can become the dominant process to produce analyte ions. In general, only low or no ion signals from very large proteins can be detected from samples of powder mixtures while strong short peptide ions were detected.

3.5. Cationization

Experimental results of peptide with gold nanoparticles are shown in Fig. 7. No protonated positive ions were detected. Ions of peptide with attached Na^+ are the primary peaks for positive ion spectrum. Since there were no organic matrices, the production of peptide ions had to be produced by collision in the gas phase. However, deprotonated peptide ions were observed in negative ion mode. Na^+ attached negative ions ($M + Na^+ - 2H^+$) were also detected.

Thus, cationization and anionization become important channels to produce ions. The incorporation of these ions can occur either in the solid or gas phase. In general, signals are often weak when cationization and anionization are required to produce MALDI ion signals.

For easy comparison, Table 1 is set up for three different models for various experimental observations.

Table 1
Different ionization models for MALDI on various experimental observations

	PI	CI	ETID
Sweet spot	No	No	Yes
Matrix-selective	No	Hard to judge	Yes
Polymer ratio	No	Yes	Yes
Laser power dependence	No	Hard to judge	Yes
Matrix suppression	No	Hard to judge	Hard to judge
Equal positive and negative ions for large biomolecules	No	No	Yes
More positive ions than negative ions for peptides	Yes	Yes	Yes
Ions from powder	Yes	No	No
Ions from nanometals	No	No	No.

In conclusion, we propose a pseudo proton transfer process for MALDI mechanism. An ETID model for the explanation of the equal amount of positive and negative ions produced during a MALDI process of large proteins and oligonucleotides. Although MALDI researchers have no good agreement on a simple model for MALDI ionization mechanism now, researchers in this field more or less consider that different ionization mechanisms simultaneously occur for MALDI of various types of compounds. From Table 1, it is clear that no model explains all observations. The proposed model can be used to explain most phenomena observed in MALDI. The proposed model in this work is intended to stimulate more discussions and studies on the MALDI mechanism. More works need to be further pursued in order to evaluate the validity of this model.

Acknowledgements

This work is supported by Genomic Research Center, Academia Sinica, Taiwan. Help on sample preparation by Ming Chia Huang and manuscript preparation by Kuan Ju Lin are also acknowledged.

References

[1] M. Karas, D. Bachmann, F. Hillenkamp, Int. J. Mass Spectrom. Ion Process. 78 (1987) 53.

[2] K. Tanaka, H. Waki, Y. Ido, S. Akita, Y. Yoshida, T. Yoshida, Rapid Commun. Mass Spectrom. 2 (1988) 151.
[3] S.F. Wong, C.K. Meng, J.B. Fenn, J. Phys. Chem. 92 (1988) 546.
[4] M. Karas, F. Hillenkamp, Anal. Chem. 60 (1988) 2299.
[5] D.L. Tabb, W.H. McDonald, J.R. Yates, J. Proteome Res. 1 (2002) 21.
[6] K. Tang, N.I. Taranenko, S.L. Allman, C.H. Chen, L.Y. Chang, K.B. Jacobson, Rapid Commun. Mass Spectrom. 8 (1994) 637.
[7] K.J. Wu, A. Steding, C.H. Becker, Rapid Commun. Mass Spectrom. 7 (1993) 142.
[8] B. Stahl, M. Steup, M. Karas, F. Hillenkamp, Anal. Chem. 63 (1993) 1463.
[9] D.J. Harvey, Mass Spectrom. Rev. 18 (1999) 349.
[10] M. Kussmann, E. Nordhoff, H. Rehbek-Nielson, S. Haebel, M. Rossel-Larsen, L. Jakobsen, J. Gobom, E. Mirgorodskaya, A. Kroll-Kristensen, L. Palm, P. Roepstorff, J. Mass Spectrom. 32 (1997) 593.
[11] P. Juhasz, C.E. Costello, K. Biemann, J. Am. Soc. Mass Spectrom. 4 (1993) 399.
[12] S. Lee, M.A. Winnik, R.M. Whittal, L. Li, Macromolecules 29 (1996) 3060.
[13] N.I. Taranenko, S.L. Allman, V.V. Golovlev, N.V. Taranenko, N.R. Isola, C.H. Chen, Nucl. Acids Res. 26 (1998) 2488.
[14] Y.F. Zhu, N.I. Taranenko, S.L. Allman, N.V. Taranenko, S.A. Martin, L.A. Haff, C.H. Chen, Rapid Commun. Mass Spectrom. 11 (1977) 897.
[15] L.Y. Chang, K. Tang, M. Schell, C. Ringelberg, K.J. Matteson, S.L. Allman, C.H. Chen, Rapid Commun. Mass Spectrom. 9 (1995) 772.
[16] N.I. Taranenko, K.J. Matteson, C.N. Chung, Y.F. Zhu, L.Y. Chang, S.L. Allman, L. Haff, S.A. Martin, C.H. Chen, Genet. Anal.: Biomol. Eng. 13 (1996) 87.
[17] N.I. Taranenko, N.T. Potter, S.L. Alolman, V.V. Golovlev, C.H. Chen, Genet. Anal.: Biomol. Eng. 15 (1999) 25.
[18] S. Trimpin, A. Rouhanipour, R. Az, H.J. Rader, K. Muller, Rapid Commun. Mass Spectrom. 15 (2001) 1364.
[19] E.F. Petricoin, A.M. Ardekani, B.A. Hitt, P.J. Levine, V.A. Fusaro, S.M. Steinberg, G.B. Mills, C. Simone, D.A. Fishman, E.C. Kohn, L.A. Liotta, Lancet: Mech. Dis. 359 (2002) 572.
[20] K. Tang, S.L. Allman, R.B. Jones, C.H. Chen, Org. Mass Spectrom. Lett. 27 (1992) 1389.
[21] K. Tang, S.L. Allman, R.B. Jones, C.H. Chen, Anal. Chem. 65 (1993) 2164.
[22] R.B. Jones, S.L. Allman, K. Tang, W.R. Garrett, C.H. Chen, Chem. Phys. Lett. 212 (1993) 451.
[23] D.J. Harvey, A.P. Hunter, B.H. Bateman, J. Brown, G. Critchley, Int. J. 188 (1999) 131.
[24] C. Sottani, M. Fiorentino, C. Minoia, Rapid Commun. Mass Spectrom. 11 (1997) 907.
[25] K. Tang, N.I. Taranenko, S.L. Allman, L.Y. Chang, C.H. Chen, Rapid Commun. Mass Spectrom. 8 (1994) 727.
[26] D.C. Schriemer, L. Li, Anal. Chem. 69 (1997) 4169.
[27] H. Ehring, M. Karas, F. Hillenkamp, Org. Mass Spectrom. 27 (1992) 427.
[28] Y. Kong, Y. Zhu, J.Y. Zhang, Rapid Commun. Mass Spectrom. 15 (2001) 57.
[29] V. Karbach, R. Knochenmuss, Rapid Commun. Mass Spectrom. 12 (1998) 968.
[30] R. Knochemuss, F. Dubois, M.J. Dale, R. Zenobi, Rapid Commun. Mass Spectrom. 10 (1996) 871.
[31] Y. Liu, X. Sun, B. Guo, Rapid Commun. Mass Spectrom. 17 (2003) 2354.
[32] R. Zenobi, R. Knochenmuss, Mass Spectrom. Rev. 17 (1998) 337.
[33] J. Krause, M. Stoeckli, U.P. Schlunegger, Rapid Commun. Mass Spectrom. 10 (1996) 1927.
[34] A.G. Harrison, Mass Spectrom. Rev. 16 (1997) 201.
[35] K. Dreisewerd, M. Schurenberg, M. Karas, F. Hillenkamp, J. Inter, Mass Spectrom. Ion Process. 154 (1996) 171.
[36] W. Lehmann, R. Knochenmuss, R. Zenobi, Rapid Commun. Mass Spectrom. 11 (1997) 1483.
[37] T.D. McCarley, R.L. McCarley, P.A. Limbach, Anal. Chem. 70 (1998) 4376.
[38] R. Kruger, A. Pfenninger, I. Fournier, M. Gluckmann, M. Karas, Anal. Chem. 73 (2001) 5812.
[39] M. Karas, M. Gluckmann, J. Schafer, J. Mass Spectrom. 35 (2000) 1.
[40] M. Karas, R. Kruger, Chem. Rev. 103 (2003) 427.
[41] A.N. Krutchinsky, A.I. Dolgunine, M.A. Khodorkovski, Anal. Chem. 67 (1995) 1963.
[42] W.P. Peng, Y.C. Yang, C.W. Lin, H.C. Chang, Anal. Chem. 77 (2005) 7084.
[43] W.P. Peng, Y.C. Yang, M.W. Kang, Y.K. Tzeng, Z. Nie, H.C. Chang, W. Chang, C.H. Chen, Angew. Chem. Int. Ed. 45 (2006) 1423.
[44] D.W. Armstrong, L. Zhang, L. He, M.L. Gross, Anal. Chem. 73 (2001) 3679.
[45] N.I. Taranenko, R. Hurt, J.Z. Zhou, N.R. Isola, H. Huang, S.H. Lee, C.H. Chen, J. Microbiol. Meth. 48 (2002) 101.
[46] P.W. Geno, R.D. MacFarlane, Int. J. Mass Spectrom. Ion Process. 92 (1989) 194.
[47] G.R. Kinsel, R.D. Edmondson, D.H. Russell, J. Mass Spectrom. 32 (1997) 714.
[48] R.A. Meyers (Ed.), Encyclopedia of Molecular Cell Biology and Molecular Medicine, vol. 7, Wiley-VCH Verlag GmbH & Co, Weinheim, Germany, 2005.
[49] W.P. Peng, Y.C. Yang, M.W. Kang, Y.T. Lee, H.C. Chang, J. Am. Chem. Soc. 126 (2004) 11766.